SD-pair shell model and the interacting boson model

Yan-An Luo,[1,2,3,*] Feng Pan,[1,2] Chairul Bahri,[2,4] and Jerry P. Draayer[2]
[1]*Department of Physics, Liaoning Normal University, Dalian 116029, P.R. China*
[2]*Department of Physics and Astronomy, Louisiana State University, Baton Rouge, Louisiana 70803, USA*
[3]*Department of Physics, Nankai University, Tianjin, 300071, People's Republic of China*
[4]*Department Fisika, FMIPA, Universitas Indonesia, Depok 16424, Indonesia*
(Received 29 December 2004; published 13 April 2005)

The *SD*-pair shell model (SDPSM) is shown to reproduce approximately typical spectra, $E2$ transition strengths, and wave functions of the U(5), SO(6), and SU(3) limits of the interacting boson model (IBM). Consequently, the analysis confirms that the IBM has a sound shell-model foundation; it also demonstrates that the truncation scheme adopted in the SDPSM is reasonable.

DOI: 10.1103/PhysRevC.71.044304 PACS number(s): 21.60.Cs, 21.60.Fw

I. INTRODUCTION

The discovery of low-lying collective modes, like vibrations and rotations, as well as higher-lying ones like giant resonances, etc., in the medium- and heavy-mass nuclei represents a significant achievement. These modes can be tied to the collective quadrupole motion of the constituent nucleons. An interesting and challenging task in nuclear theory is to describe these collective modes in terms of *fermion* degrees of freedom. Since truly large-space shell-model calculations remain out of reach, even with the best of modern computational facilities, one has to evoke some type of truncation scheme. The crucial issue is how to truncate a huge shell-model space to a manageable and effective subspace so that calculations within the subspace are both feasible and realistic, thereby providing a sound understanding of the collective degrees of freedom that are at play. The success of the interacting boson model (IBM) [1] suggests that S and D pairs play a dominant role in the spectroscopy of low-lying nuclear modes [2–4]. Although the size of the S-D subspace is typically only 10^2–10^3 and therefore not difficult to manage, the calculation of matrix elements in a "realistic" S-D subspace is not simple because the subspace is not closed under the action of pair annihilation operators. This renders the usual coefficient of fractional parentage (CFP) technique inapplicable. To circumvent this difficulty, in the interacting boson model the S and D fermion pair operators are treated approximately as s and d bosons through a so-called Otsuka, Arima, and Iachello (OAI) mapping procedure [5].

Studies focused on exploring the microscopic foundation of the IBM using various mapping procedures have extended over nearly two decades [4–15]. In these studies, the s and d bosons are considered to correspond to collective S and D pairs of valencelike nucleons [5–7,16]. By using the generalized Wick theorem for fermion clusters [17], the nucleon-pair shell model (NPSM) has been proposed for nuclear collective motion in which collective nucleon pairs with various angular momenta serve as the building blocks [18]. The NPSM has the advantages that the normal and abnormal parity orbits can be treated on the same footing, which is flexible enough to include the broken pair approximation [19], the pseudo SU(2) or the favored pair model [20], and the fermion dynamical symmetry model (FDSM) [21] as special cases; it also allows various truncation schemes ranging from the truncation to the S-D subspace up to the full shell-model space. Because the computational time increases dramatically with the size of the subspace, one normally truncates this shell-model space for medium- and heavy-mass nuclei to the collective S-D subspace. The latter is called the *SD*-pair shell model (SDPSM). In the SDPSM, the Hamiltonian is diagonalized exactly in the S-D space. It is the aim of this paper to study whether the SDPSM can reproduce the vibrational, rotational, and γ-unstable spectra corresponding to those of U(5), SU(3), and SO(6) limits of the IBM.

The paper is organized as follows. Section II is devoted to a brief review of the model. The results corresponding to the three limiting cases are discussed in Sec. III–V. Section VI gives a short summary of the results.

II. THE MODEL

Though the general model Hamiltonian can be treated within the SDPSM [18], we use a simpler Hamiltonian to see if the typical spectra in the IBM could be reproduced. The Hamiltonian chosen is

$$\begin{aligned} H &= H_\pi + H_\nu + H_{\pi\nu}, \\ H_\sigma &= H_\sigma(0) - G_\sigma \mathcal{S}^\dagger(\sigma)\mathcal{S}(\sigma) - \kappa_\sigma Q_\sigma^2 \cdot Q_\sigma^2, \\ H_\sigma(0) &= \sum_{\sigma a} \epsilon_{\sigma a} n_{\sigma a}, \qquad \sigma = \pi, \nu, \\ H_{\pi\nu} &= -\kappa Q_\pi^2 \cdot Q_\nu^2, \\ \mathcal{S}^\dagger &= \sum_a \frac{\widehat{a}}{2}\left(C_a^\dagger \times C_a^\dagger\right)_0^0, \qquad \widehat{a} = \sqrt{2a+1}, \\ Q_\mu^2 &= \sqrt{16\pi/5}\sum_{i=1}^{n} r_i^2 Y_{2\mu}(\theta_i \phi_i), \end{aligned} \tag{1}$$

*Electronic address: luoya@nankai.edu.cn

where $\epsilon_{\sigma\alpha}, G_\sigma, \kappa_\sigma$, and κ are the single-particle energy of the αth level, the pairing interaction strength, the quadrupole-quadrupole interaction strength among like nucleons, and the quadrupole-quadrupole interaction strength between protons and neutrons, respectively, which emphasizes pairing and quadrupole-quadrupole interactions. The $E2$ transition operator is

$$T(E2) = e_\pi Q_\pi^2 + e_\nu Q_\nu^2, \tag{2}$$

where e_ν and e_π are the effective charges of the neutron and proton, respectively.

The collective pairs $A_\mu^{r\dagger}$ with $r = 0, 2$ and the angular momentum projection μ built from many noncollective pairs $(C_a^\dagger \times C_b^\dagger)_\mu^r$ in the single-particle levels a and b are

$$\begin{aligned} A_\mu^{r\dagger} &= \sum_{ab} y(abr)\big(C_a^\dagger \times C_b^\dagger\big)_\mu^r, \\ y(abr) &= -\theta(abr)y(bar), \quad \theta(abr) = (-)^{a+b+r}, \end{aligned} \tag{3}$$

where $y(abr)$ are structure coefficients. There are many ways to determine the S and D pairs [4,6,7,9–16]. In this paper, as an approximation, the S-pair structure coefficients are determined as $y(aa0) = \sqrt{2a+1}\frac{v_a}{u_a}$, where v_a and u_a are the occupied and unoccupied amplitudes for orbit a obtained by solving the associated BCS equation. The D pair [22] is obtained by using the commutator,

$$D^\dagger = \tfrac{1}{2}[Q^2, S^\dagger] = \sum_{ab} y(ab2)\big(C_a^\dagger \times C_b^\dagger\big)^2. \tag{4}$$

A nonorthonormal N-pair state is given by

$$\begin{aligned} A_{M_N}^{J_N\dagger}(r_i, J_i) = A_{M_N}^{J_N\dagger} = (\cdots((A^{r_1\dagger} \times A^{r_2\dagger})^{J_2} A^{r_3\dagger})^{J_3} \\ \times \cdots \times A^{r_N\dagger})_{M_N}^{J_N}, \end{aligned} \tag{5}$$

with the convention that $r_1 \equiv J_1$, and $r_1 \geqslant r_2 \geqslant \ldots \geqslant r_N$. For a given set of quantum numbers $(r_1 r_2 \ldots r_N : J_N M_N)$, not all sets of intermediate angular momenta $J_2 \ldots J_{N-1}$ lead to independent or orthogonal basis states. To address this over-completeness issue, for a given J_N, we take the independent sets formed by choosing the largest possible intermediate angular momentum values J_i. This choice reduces the number of intermediate summations required and makes it a relatively easy matter to identify the linearly independent, but still nonorthogonal, many-pair basis states. For example, for a configuration with four D pairs, the independent but nonorthonormal basis vectors can be chosen as

$$\begin{aligned} &|(D^\dagger)^4(S^\dagger)^{N-4}, J_1 J_2 J_3 \cdots J_N\rangle, \\ &J_1 J_2 J_3 J_4 = 2420, 2432, 2442, 2444, 2464, 2465, 2466, 2468. \end{aligned} \tag{6}$$

A recursion formula for the overlap between two N-pair states is

$$\begin{aligned} &\langle s_1 s_2 \cdots s_N; J_1' \cdots J_{N-1}' J_N | r_1 r_2 \cdots r_N; J_1 \cdots J_N\rangle \\ &= (\hat{J}_{N-1}'/\hat{J}_N)(-)^{J_N + s_N - J_{N-1}'} \sum_{k=N}^{1} \sum_{L_{k-1}\cdots L_{N-1}} H_N(s_N)\cdots H_{k+1}(s_N) \\ &\times \Bigg[\psi_k \delta_{L_{k-1}, J_{k-1}} \langle s_1 \cdots s_{N-1}; J_1' \cdots J_{N-1}' | r_1 \cdots r_{k-1}, r_{k+1} \cdots r_N; J_1 \cdots J_{k-1} L_k \cdots L_{N-1}\rangle \\ &+ \sum_{i=k-1}^{1} \sum_{r_i' L_i \cdots L_{k-2}} \langle s_1 \cdots s_{N-1}; J_1' \cdots J_{N-1}' | r_1 \cdots r_i' \cdots r_{k-1}, r_{k+1} \cdots r_N; J_1 \cdots J_{i-1} L_i \cdots L_{N-1}\rangle \Bigg], \end{aligned} \tag{7}$$

where $\hat{J} = \sqrt{2J+1}$, $H_k(s_N)$ is essentially a Racah coefficient, ψ_k is a constant depending on the structure of the pairs $A^{r_k\dagger}$ and $A^{s_N\dagger}$, while r_i' represents a new collective pair $A^{r_i'\dagger}$ with a new distribution function $y'(a_k a_i r_i')$ depending on the structure of the pair $A^{r_k\dagger}$, $A^{r_i\dagger}$ and $A^{s_N\dagger}$, and the intermediate quantum numbers $L_i \cdots L_{k-2} L_{k-1}$. The $L_{i'} (i' = i, \ldots, k-2, k-1)$ is the angular momentum of the first i' pairs in the bra vector on the right-hand side of Eq. (7). Since the right-hand side of Eq. (7) is a linear combination of overlaps for $N-1$ pairs, all overlaps can be calculated recursively starting from the simplest two-particle configuration. The details of the model can be found in Refs. [18,23,24].

To show that the SDPSM can produce the limiting cases of the IBM, the theory was applied to spectrum and $E2$ transition rates. From [23,25–29] we know that explicit expressions for wave functions expanded in terms of a linear combination of the nonorthogonal (but normalized) multipair basis states are helpful in providing a microscopic description of the states. Thus, the wave functions for some cases were also studied and the results are given below. The following shorthand notation is used for the multipair states:

$$\begin{aligned} &\big|\big(D_\pi^\dagger\big)^{n_\pi}\big(S_\pi^\dagger\big)^{N_\pi - n_\pi}\big(D_\nu^\dagger\big)^{n_\nu}\big(S_\nu^\dagger\big)^{N_\nu - n_\nu}; JM\big\rangle \\ &\to |(D_\nu)^{n_\nu}(D_\pi)^{n_\pi}; JM\rangle, \big|\big(S_\pi^\dagger\big)^{N_\pi}\big(S_\nu^\dagger\big)^{N_\nu}; JM\big\rangle \to |S; JM\rangle. \end{aligned}$$

We will also use brackets for those multipair basis states that occur more than once and which are distinguished by the value of intermediate angular momentum.

III. VIBRATIONAL LIMIT

To see whether the vibrational spectrum of the IBM can be reproduced within the SDPSM, the proton-neutron coupled

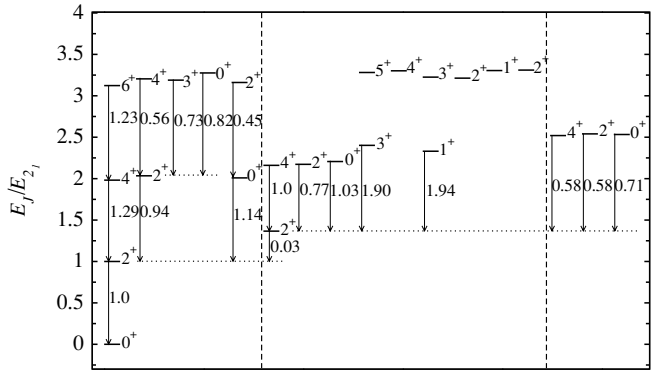

FIG. 1. The vibrational spectrum of the SDPSM. Some relative $B(E2)$ ratios are also shown with the effective charges fixed at $e_\pi = 1.5\,e$ and $e_\nu = 0.5\,e$.

system with a 2π-2ν pair was studied. We restricted ourselves to the 50–82 shell with the same set of orbits taken for both the protons and neutrons. The single-particle energies that we used are from Ref. [30] with the same values used in both the proton and neutron sectors, namely, 2.99, 2.69, 0.963, 0.0, and 2.76 MeV for $j = 1/2, 3/2, , 5/2, 7/2$, and $11/2$ levels, respectively. The pairing interaction strengths for proton and neutron were assumed, for simplicity, to be the same with $G_\pi = G_\nu \cong G = 0.3$ MeV, and $\kappa_\pi = \kappa_\nu = 0$. By fitting $E_{4_1^+}/E_{2_1^+} = 2.0$, κ was fixed at 0.01 MeV/r_0^4 with the oscillator length $r_0 = \sqrt{\hbar/m\omega}$.

To show the vibrational pattern that we obtained, some low-lying states divided by $E_{2_1^+}$ for normalization purposes are presented in Fig. 1. As expected, the results show that the states are grouped like those in the $\mathrm{U}_\pi(5)\otimes \mathrm{U}_\nu(5)$ symmetry in the IBM-II [1]. For example, as shown in the left panel, the 2_3^+ and 0_2^+ states are degenerate with the 4_1^+ state. Figure 1 also shows that these groups are equally spaced, which is a typical feature of the U(5) limit in the IBM.

Wave functions for a few important states are given in Table I, which shows that the 0_1^+ state is almost a pure *S*-pair state with an *S*-pair component equal to 0.9926; both 2_1^+ and 2_2^+ states are one-*D*-pair states, but the two components in the 2_1^+ state are coherent with the same phase, while they are incoherent with the opposite phase for the 2_2^+ state; the 4_1^+, 2_3^+, and 0_2^+ states are all basically two-*D*-pair states; and the 6_1^+ state is a three-*D*-pair state. In addition to the spectrum, the $E2$ transition can be used to probe the collectivity of low-lying states. The relative $B(E2)$ ratios for some low-lying states are also presented in Fig. 1, which indicates that the strong $E2$ transitions occur between states with D^n and those with D^{n-1} in agreement with the detailed structure of the wave functions. For instance, the two-*D*-pair states, 4_1^+, 2_3^+, and 0_2^+, mainly deexcite to the one-*D*-pair 2_1^+ state, which is a typical feature in the vibrational limit. The $B(E2)$ ratios are 1.29, 0.94, and 1.14 for $\frac{B(E2;4_1^+\to 2_1^+)}{B(E2;2_1^+\to 0_1^+)}$, $\frac{B(E2;2_2^+\to 2_1^+)}{B(E2;2_1^+\to 0_1^+)}$, and $\frac{B(E2;0_2^+\to 2_1^+)}{B(E2;2_1^+\to 0_1^+)}$, respectively. One can also see that the $E2$ transition from the 2_2^+ to the 2_1^+ state is depressed since the 2_2^+ state is also a one-*D*-pair state with $\frac{B(E2;2_2^+\to 2_1^+)}{B(E2;2_1^+\to 0_1^+)} = 0.03$.

IV. γ-UNSTABLE LIMIT

From the periodic chart, one can deduce that nuclei that display an SO(6) spectrum lie close to the end of the shell, at least in the neutron sector. ^{132}Ba, which is a 3π-$3\bar{\nu}$ pair system, is an example. Therefore, to explore whether the γ-unstable spectrum can be realized in the SDPSM, we considered the same system as in the vibrational limit in the 50–82 shell, with the same set of orbits taken for both the protons and neutrons. The single-particle energies were also taken to be the same as those used in the vibrational limit. As discussed in Ref. [31], since the SO(6) nuclei in the 50–82 shell are those with a valence neutron number close to the end of the shell, neutron pairs in this case were treated as two neutron-hole pairs, and

TABLE I. Main components of selected eigenstates for the vibrational and γ-soft cases. Only components with amplitudes larger than 0.2 are shown.

U(5)	State	S	D_ν	D_π	$D_\pi D_\nu$	D_ν^2	D_π^2	$D_\pi^2 D_\nu$	$D_\nu^2 D_\pi$	$D_\nu^2 D_\pi^2$
	0_1^+	0.9926								
	0_2^+				0.5914	0.5774	0.5774			
	2_1^+		0.7044	0.7044						
	2_2^+		0.6933	−0.6933						
	2_3^+				0.5096	0.6017	0.6017			
	4_1^+				0.5668	0.5781	0.5781			
	6_1^+							0.7010	0.7010	
SO(6)	0_1^+	0.8967			−0.5972					
	0_2^+					−0.4979	0.4979	−0.5395	0.5395	
	2_1^+		−0.6747	0.6747				−0.2586	0.2586	
	2_2^+		0.3233	0.3233	−0.6516	0.3718	0.3718			
	4_1^+				−0.6786	0.5252	0.5252			
	6_1^+							−0.7029	0.7029	

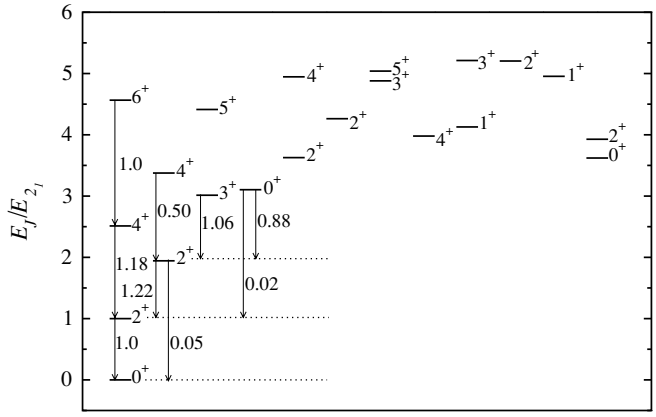

FIG. 2. The γ-unstable spectrum. Some relative $B(E2)$ ratios are also shown with the effective charges fixed at $e_\pi = 1.5\,e$ and $e_\nu = 0.5\,e$.

a negative κ parameter was used in [31]. With the pairing strength fixed as $G_\pi = G_\nu \cong G = 0.2$ MeV and $\kappa_\pi = \kappa_\nu = 0$, the κ was fixed to be -0.06 MeV$/r_0^4$ by fitting the energy ratio $E_{4_1^+}/E_{2_1^+} = 2.5$. The excitation energies divided by $E_{2_1^+}$ are given in Fig. 2, which shows that the 2_2^+ state is lower than the 4_1^+ and 0_2^+ states, and the 0_2^+ state is higher than the 4_1^+ and 2_2^+ states. Clearly, the level patterns of the γ-unstable spectrum for the $\mathrm{SO}_\pi(6) \otimes \mathrm{SO}_\nu(6)$ symmetry in the IBM-II [1] are well reproduced in the SDPSM.

Wave functions for a few important states in this case are also given in Table I, which shows that the multi-D-pair components are mixed more strongly with each other than in the vibrational limit. In the ground state, the pure S-pair and $D_\pi D_\nu$ components are dominant with amplitudes 0.8967 and -0.5972, respectively. Furthermore, in the γ-unstable case, the 2_1^+, 4_1^+, and 6_1^+ states are one-, two-, and three-D-pair states, respectively, while the 2_2^+ state is essentially a two-D-pair state. Table I also shows that the 0_2^+ state in the γ-unstable case is mainly three-D pairs. $E2$ transitions for some important low-lying states are also shown in Fig. 2. Again, the $E2$ transitions are consistent with the detailed structure of the wave functions; namely, strong $E2$ transition occurs between states with a D^n configuration and those with a D^{n-1} configuration. The relative $B(E2)$ ratio $\frac{B(E2;4_1^+\to 2_1^+)}{B(E2;2_1^+\to 0_1^+)} = 1.183$ and 1.0 between the 6_1^+ and the 4_1^+ states; the 2_2^+ state mainly deexcites to the 2_1^+ state with a ratio 1.22, while it is forbidden from deexciting to the 0_1^+ state because the D-pair number difference between the two states is 2. Figure 2 also shows that the $E2$ transition between the 0_2^+ state and the 2_2^+ state is dominant over that between the 0_2^+ and 2_1^+ states, which is another typical feature of the γ-unstable limit of the corresponding IBM theory. Other results include the $\frac{B(E2;0_2^+\to 2_2^+)}{B(E2;2_1^+\to 0_1^+)} = 0.88$, while the ratio is 0.02 between the 0_2^+ and 2_1^- states.

V. ROTATIONAL LIMIT

To see whether the rotational limit of the IBM can be realized within the SDPSM, a pure quadrupole-quadrupole interaction with $\kappa_\pi = \kappa_\nu = \frac{1}{2}\kappa$ was used in the 3π-3ν pair system of the *gds* shell. In this case, we assume the single-particle energy levels are degenerate with

$$H = -\tfrac{1}{2}\kappa\left(Q_\pi^2 + Q_\nu^2\right)\cdot\left(Q_\pi^2 + Q_\nu^2\right). \tag{8}$$

Though a more sophisticated Hamiltonian can also be adopted, the Hamiltonian (8) is suitable to emphasize the quadrupole-quadrupole interaction in this limiting case. The S-pair structure coefficient was fixed by $y(aa0) = \widehat{a}(\frac{N}{\Omega_a - N})^{1/2}$, where Ω_a is defined as $\Omega_a = a + 1/2$ and N is the number of like-nucleon pairs; the D pair was determined by commutator (4). The energy ratios of the ground band for this system are shown in row (A) of Table II for the quadrupole-quadrupole interaction strength fixed as $\kappa = 0.01\,\mathrm{MeV}/r_0^4$. Some low-lying states are shown in Fig. 3, in which the levels are arranged into bands. It is clear, as shown in Ref. [3], that the rotational level pattern can be reproduced very well in the SDPSM [1] for this case. From Fig. 3, one can also see that the 2_3^+ and 2_4^+ bands are lower than the 2_5^+ band, the so-called γ band of the Bohr-Mottelson model. If we switch on the $L\cdot L$ term with another parameter, the rotational level pattern will obviously improve. To track the rotational pattern more closely, we also show the energies of the ground, 1_1^+, 0_2^+, and 2_5^+ bands plotted as a function of $J(J+1)$ in Fig. 4. The linearity of the results shows that these bands vary with $J(J+1)$, a clear signature of their rotational character. Also note that the 0_2^+ and 2_5^+ bands are almost degenerate, which is close to what occurs in the SU(3) limit of the IBM.

It is interesting to compare the wave functions of the rotational limit with those of the vibrational and γ-unstable limits. A few important states are presented in Table III.

TABLE II. Energy ratios $E_{J_1^+}/E_{2_1^+}$.

	$J=4$	$J=6$	$J=8$	$J=10$	$J=12$
(A)	3.33	6.96	11.88	18.06	25.48
(B)	3.18	6.41	10.58	15.55	21.17
(C)	3.31	6.87	11.63	17.53	24.51
IBM-SU(3)	3.33	7.0	12.0	18.25	26.0

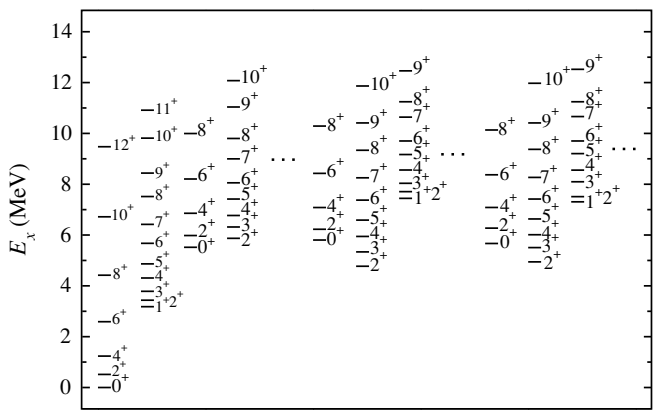

FIG. 3. Rotational spectrum for the coupled proton-neutron system in the SDPSM.

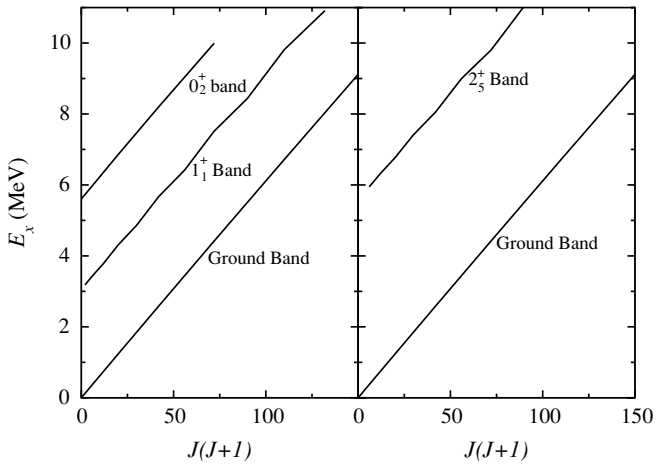

FIG. 4. Energies of the ground, 1_1^+, 2_5^+, and 0_2^+ bands plotted as a function of $J(J+1)$.

The results show that all the states in the rotational limit are mixtures of multi-*D*-pair components, and the contribution from each component is more or less the same. Hence, no component can be ignored. The results clearly show that strong deformation leads to strong mixture of the multi-*D*-pair components in the SDPSM.

Some relative $B(E2)$ ratios for this limit are listed in Table IV. The results clearly show that interband transitions are much stronger than intraband transitions. For example, $\frac{B(E2;4_1^+\to 2_1^+)}{B(E2;2_1^+\to 0_1^+)} = 1.346$, while it is almost zero from the 2_2^+ to the 2_1^+ and the 0_2^+ to the 2_1^+ states with $\frac{B(E2;2_2^+\to 2_1^+)}{B(E2;2_1^+\to 0_1^+)} = 0.009$ and $\frac{B(E2;2_2^+\to 2_1^+)}{B(E2;2_1^+\to 0_1^+)} = 0.001$. These are comparable to the corresponding typical $E2$ transitions in the rotational limit.

Similar calculations to those for the *gds* shell were performed for the 50–82 shell, and the results are given in row (B) of Table II. It is clear that the rotational level pattern cannot be as well reproduced in this case because the particles in the $h_{11/2}$ intruder level cannot couple with those in the normal parity levels to form the positive parity pairs as discussed in Ref. [32].

The mean field and the pairing interactions in (2) were neglected in reproducing the rotational spectrum previously because, as is known, these terms tend to reduce the deformation. To explore their effect, the *gds* shell was also investigated with the full Hamiltonian given in (2). The single-particle energies used in the vibrational and γ-unstable limit were also used here except $\epsilon_{h_{11/2}} = 2.76$ MeV was replaced by $\epsilon_{g_{9/2}} = 0$ MeV, since in the real case $g_{9/2}$ lies lowest in the *gds* shell. For simplicity, we set $G_\pi = G_\nu = 0.3$ MeV and $2\kappa_\pi = 2\kappa_\nu = \kappa = 0.5$ MeV/r_0^4. The results for the ground-state band are given in row (C) of Table II, which shows that the rotational level pattern can still be realized approximately, even with the inclusion of realistic single-particle energies and the pairing interactions, under the condition that the quadrupole-quadrupole interaction remains the dominant interaction.

VI. SUMMARY

In summary, the vibrational, γ-unstable, and rotational spectra corresponding to the U(5), SO(6), and SU(3) limiting cases in the IBM can indeed be reproduced in the nucleon-pair shell model truncated to an *S*-*D* subspace (SDPSM). The analysis not only shows that the IBM has a sound shell-model foundation, but also confirms that the truncation scheme adopted in the *SD*-pair shell model seems reasonable as long as the Hamiltonian is reasonably chosen even when realistic single-particle energies are taken into consideration. The results suggest the value of further analysis using the SDPSM to see whether shape phase transitions could be described in terms of the nucleon degrees of freedom. Refs. [33,34] show that there are critical point symmetries such as X_5 and E_5 predicted from the Bohr Hamiltonian. It should be an interesting exercise to describe such critical point phenomena within the framework of the SDPSM with its fermion foundation.

TABLE III. Main components of some eigenstates in the rotational limit of the system with $N_\pi = N_\nu = 3$. Only components with amplitude larger than 0.25 are shown.

State	S	D_ν	D_π	$D_\pi D_\nu$	D_ν^2	D_π^2	$D_\pi^2 D_\nu$	$D_\nu^2 D_\pi$	$D_\nu^2 D_\pi^2$	$D_\nu^3 D_\pi$	$D_\pi^3 D_\nu$	$D_\pi^2 D_\nu^3$	$D_\pi^3 D_\nu^2$	$D_\pi^3 D_\nu^3$
0_1^+	0.3801			0.6489	0.3787	0.3787	0.4127	0.4127	0.3786 (0.2705) (0.3679)	0.3349	0.3349			
0_2^+	−0.3406				0.3680	0.3680			−0.6714 (0.4003)			−0.4080	−0.4080	−0.4225
2_1^+		0.3680	0.3680	0.3840			0.3675 (0.3361)	0.3675 (0.3361)	0.2586					
2_2^+							−0.4974	0.4974	0.3306 (−0.3306)	0.2852	−0.2852	−0.2617 0.2794	0.2617 −0.2794	
4_1^+				0.4918	0.3074	0.3074	0.3189 (0.3065)	0.3189 (0.3065)	0.3080 (0.3080)	0.2558	0.2558			
6_1^+							0.5058	0.5058	0.3307 (0.3307) (0.2961)	0.2839	0.2839	0.2648	0.2648	

TABLE IV. A part of relative $B(E2)$ ratios in the rotational spectrum for the system with $N_\pi = N_\nu = 3$. The effective charges were fixed as $e_\pi = 3e_\nu = 1.5\,e$.

$\frac{J_i^+ \to J_f^+}{2_1^+ \to 0_1^+}$		$\frac{J_i^+ \to J_f^+}{3_1^+ \to 1_1^+}$		$\frac{J_i^+ \to J_f^+}{2_6^+ \to 0_2^+}$		$\frac{J_i^+ \to J_f^+}{4_5^+ \to 2_5^+}$	
$4_1^+ \to 2_1^+$	1.346	$4_2^+ \to 2_2^+$	1.112	$4_6^+ \to 2_6^+$	1.129	$5_4^+ \to 3_4^+$	1.003
$6_1^+ \to 4_1^+$	1.319	$6_2^+ \to 4_2^+$	1.163	$6_6^+ \to 4_6^+$	1.026	$6_5^+ \to 4_5^+$	1.556
$8_1^+ \to 6_1^+$	1.138	$5_1^+ \to 3_1^+$	1.439	$8_6^+ \to 6_6^+$	0.707	$7_4^+ \to 5_4^+$	1.049
$2_2^+ \to 2_1^+$	0.009	$7_1^+ \to 5_1^+$	1.356			$8_5^+ \to 6_5^+$	1.323
$0_2^+ \to 2_1^+$	0.001	$8_2^+ \to 6_2^+$	0.933				

ACKNOWLEDGMENTS

Support from the U.S. National Science Foundation (0140300), the Southeastern Universities Research Association, the Natural Science Foundation of China (10305006), the Education Department of Liaoning Province (202122024), and the LSU–LNNU joint research program (C164063) is acknowledged.

[1] F. Iachello and A. Arima, *The Interacting Boson Model* (Cambridge University Press, Cambridge, 1987).
[2] J. B. McGrory, Phys. Rev. Lett. **41**, 533 (1978).
[3] T. Otsuka, Nucl. Phys. **A368**, 244 (1981).
[4] P. Halse, L. Jaqua, and B. R. Barrett, Phys. Rev. C **40**, 968 (1989).
[5] T. Otsuka, A. Arima, and F. Iachello, Nucl. Phys. **A309**, 1 (1978).
[6] T. Otsuka, T. Mizusaki, and K. H. Kim, in International Conference on Perspectives for the Interacting Boson Model, Padova, Italy, 1994, edited by R. F. Casten *et al*. (World Scientific, Singapore, 1994), p. 33.
[7] T. Mizusaki and T. Otsuka, Prog. Theor. Phys. Suppl. **125**, 97 (1996).
[8] S. Pittel, P. D. Duval, and B. R. Barrett, Ann. Phys. (NY) **144**, 168 (1982).
[9] A. Klein and M. Vallieres, Phys. Lett. **B98**, 5 (1981).
[10] Y. K. Gambhir, P. Ring, and P. Schuck, Nucl. Phys. **A384**, 37 (1982).
[11] M. R. Zirnbauer and D. N. Brink, Nucl. Phys. **A384**, 1 (1982).
[12] E. Magline *et al*., Nucl. Phys. **A397**, 102 (1983).
[13] L. M. Yang, Z. N. Zhou, and D. H. Lu, Phys. Rev. C **40**, 2885 (1989).
[14] L. C. De Winter, N. R. Walet, P. J. Brussaard, K. Allaart, and A. E. L. Dieperink, Phys. Lett. **179**, 322 (1986).
[15] O. Scholten, Phys. Rev C **28**, 1783 (1983).
[16] T. Otsuka, A. Arima, F. Iachello, and I. Talmi, Phys. Lett. **B76**, 139 (1978).
[17] J. Q. Chen, Nucl. Phys. **A562**, 218 (1993).
[18] J. Q. Chen, Nucl. Phys. **A626**, 686 (1997).
[19] K. Allaart, E. Boeker, G. Bonsignori, M. Savoia, and Y. K. Gambhir, Phys. Rep. **169**, 209 (1988).
[20] K. T. Hecht, J. B. McGrory, and J. P. Draayer, Nucl. Phys. **A197**, 369 (1972).
[21] C. L. Wu, D. H. Feng, X. G. Chen, J. Q. Chen, and M. Guidry, Phys. Rev. C **36**, 1157 (1987).
[22] I. Talmi, Nucl. Phys. **A172**, 1 (1972).
[23] J.-Q. Chen and Y.-A. Luo, Nucl. Phys. **A639**, 615 (1998).
[24] Y. M. Zhao, N. Yoshinaga, S. Yamaji, J. Q. Chen, and A. Arima, Phys. Rev. C **62**, 014304 (2000).
[25] Y. A. Luo, J. Q. Chen, and J. P. Draayer, Nucl. Phys. **A669**, 101 (2000).
[26] Y. A. Luo, J. Q. Chen, Y. C. Gao, P. Z. Ning, and J. P. Draayer, Chin. Phys. Lett. **18**, 501 (2001).
[27] Y. A. Luo, X. B. Zhang, F. Pan, P. Z. Ning, and J. P. Draayer, Phys. Rev. C **64**, 047302 (2001).
[28] Y. A. Luo and J. Q. Chen, Phys. Rev. C **58**, 589 (1998).
[29] Y. A. Luo, J. Q. Chen, T. F. Feng, and P. Z. Ning, Phys. Rev. C **64**, 037303 (2001).
[30] B. Fogelberg and J. Blomqvist, Nucl. Phys. **A429**, 205 (1984).
[31] T. Otsuka, Phys. Rev. Lett. **46**, 710 (1981).
[32] Y. A. Luo, C. Bahri, F. Pan, and J. P. Draayer, Int. J. Mod. Phys. E (accepted for publication).
[33] R. F. Casten and N. V. Zamfir, Phys. Rev. Lett. **85**, 3584 (2000).
[34] R. F. Casten and N. V. Zamfir, Phys. Rev. Lett. **87**, 052503 (2001).